

Nature of phase transition in magnetic thin films

X. T. Pham Phu^a, V. Thanh Ngo^{b,c} and H. T. Diep^{a*}

^a *Laboratoire de Physique Théorique et Modélisation, CNRS-Université de Cergy-Pontoise, UMR 8089
2, Avenue Adolphe Chauvin, 95302 Cergy-Pontoise Cedex, France*

^b *Institute of Physics, P.O. Box 429, Bo Ho, Hanoi 10000, Vietnam*

^c *Asia Pacific Center for Theoretical Physics, Hogil Kim Memorial Building 5th floor,
POSTECH, Hyoja-dong, Namgu, Pohang 790-784, Korea*

We study the critical behavior of magnetic thin films as a function of the film thickness. We use the ferromagnetic Ising model with the high-resolution multiple histogram Monte Carlo (MC) simulation. We show that though the 2D behavior remains dominant at small thicknesses, there is a systematic continuous deviation of the critical exponents from their 2D values. We observe that in the same range of varying thickness the deviation of the exponent ν is very small from its 2D value, while exponent β suffers a larger deviation. Moreover, as long as the film thickness is fixed, i. e. no finite size scaling is done in the z direction perpendicular to the film, the 3D values of the critical exponents cannot be attained even with very large (but fixed) thickness. The crossover to 3D universality class cannot therefore take place without finite size scaling applied in the z direction, in the limit of numerically accessible thicknesses. From values of exponent α obtained by MC, we estimate the effective dimension of the system. We conclude that with regard to the critical behavior, thin films behave as systems with effective dimension between 2 and 3.

PACS numbers: 75.70.Rf Surface magnetism ; 75.40.Mg Numerical simulation studies ; 64.60.Fr Equilibrium properties near critical points, critical exponents

I. INTRODUCTION

During the last 30 years, physics of surfaces and objects of nanometric size have attracted an immense interest. This is due to important applications in industry.^{1,2} An example is the so-called giant magneto-resistance (GMR) used in data storage devices, magnetic sensors, ...^{3,4,5,6} In parallel to these experimental developments, much theoretical effort^{7,8} has also been devoted to the search of physical mechanisms lying behind new properties found in nanoscale objects such as ultrathin films, ultrafine particles, quantum dots, spintronic devices etc. This effort aimed not only at providing explanations for experimental observations but also at predicting new effects for future experiments.

The physics of two-dimensional (2D) systems is very exciting. Some of those 2D systems can be exactly solved: one famous example is the Ising model on the square lattice which has been solved by Onsager.⁹ This model shows a phase transition at a finite temperature T_c given by $\sinh^2(2J/k_B T_c) = 1$ where J is the nearest-neighbor (NN) interaction. Another interesting result is the absence of long-range ordering at finite temperatures for the continuous spin models (XY and Heisenberg models) in 2D.¹⁰ In general, three-dimensional (3D) systems for any spin models cannot be unfortunately solved. However, several methods in the theory of phase transitions and critical phenomena can be used to calculate the critical behaviors of these systems.¹¹

This paper deals with systems between 2D and

3D. Many theoretical studies have been devoted to thermodynamic properties of thin films, magnetic multilayers,...^{7,8,12,13,14} In spite of this, several points are still not yet understood. We study here the critical behavior of thin films with a finite thickness. It is known a long time ago that the presence of a surface in magnetic materials can give rise to surface spin-waves which are localized in the vicinity of the surface.¹⁵ These localized modes may be acoustic with a low-lying energy or optical with a high energy, in the spin-wave spectrum. Low-lying energy modes contribute to reduce in general surface magnetization at finite temperatures. One of the consequences is the surface disordering which may occur at a temperature lower than that for interior magnetization.¹⁶ The existence of low-lying surface modes depends on the lattice structure, the surface orientation, the surface parameters, surface conditions (impurities, roughness, ...) etc. There are two interesting cases: in the first case a surface transition occurs at a temperature distinct from that of the interior spins and in the second case the surface transition coincides with the interior one, i. e. existence of a single transition. Theory of critical phenomena at surfaces^{7,8} and Monte Carlo (MC) simulations^{17,18} of critical behavior of the surface-layer magnetization at the extraordinary transition in the three-dimensional Ising model have been carried out. These works suggested several scenarios in which the nature of the surface transition and the transition in thin films depends on many factors in particular on the symmetry of the Hamiltonian and on surface parameters.

The aim of this paper is to investigate the effect of the film thickness on the critical behavior of the system. We would like to see in particular how the thickness affects the values of critical exponents. To carry

*Corresponding author, E-mail:diep@u-cergy.fr

out these purposes, we shall use MC simulations with highly accurate multiple histogram technique.^{19,20,21} We consider here the case of a simple cubic film with Ising model. For our purpose, we suppose all interactions are the same even that at the surface. This case is the simplest case where there is no surface-localized spin-wave modes and there is only a single phase transition at a temperature for the whole system (no separate surface phase transition).^{15,16} Other complicated cases will be left for future investigations. However, some preliminary discussions on this point for complicated surfaces have been reported in some of our previous papers.^{22,23}

The paper is organized as follows. Section II is devoted to a description of the model and method. Results are shown and discussed in section III. Concluding remarks are given in section IV.

II. MODEL AND METHOD

A. Model

Let us consider the Ising spin model on a film made from a ferromagnetic simple cubic lattice. The size of the film is $L \times L \times N_z$. We apply the periodic boundary conditions (PBC) in the xy planes to simulate an infinite xy dimension. The z direction is limited by the film thickness N_z . If $N_z = 1$ then one has a 2D square lattice.

The Hamiltonian is given by

$$\mathcal{H} = - \sum_{\langle i,j \rangle} J_{i,j} \sigma_i \cdot \sigma_j \quad (1)$$

where σ_i is the Ising spin of magnitude 1 occupying the lattice site i , $\sum_{\langle i,j \rangle}$ indicates the sum over the NN spin pairs σ_i and σ_j .

In the following, the interaction between two NN surface spins is denoted by J_s , while all other interactions are supposed to be ferromagnetic and all equal to $J = 1$ for simplicity. Let us note in passing that in the semi-infinite crystal the surface phase transition occurs at the bulk transition temperature when $J_s \simeq 1.52J$. This point is called "extraordinary phase transition" which is characterized by some particular critical exponents.^{17,18} In the case of thin films, i. e. N_z is finite, it has been theoretically shown that when $J_s = 1$ the bulk behavior is observed when the thickness becomes larger than a few dozens of atomic layers:¹⁵ surface effects are insignificant on thermodynamic properties such as the value of the critical temperature, the mean value of magnetization at a given T , ... When J_s is smaller than J , surface magnetization is destroyed at a temperature lower than that for bulk spins.¹⁶ However, it should be stressed that, except at the so-called "extraordinary phase transition",^{17,18} the surface criticality has not been studied as a function of the film thickness.

B. Multiple histogram technique

The multiple histogram technique is known to reproduce with very high accuracy the critical exponents of second order phase transitions.^{19,20,21}

The overall probability distribution²⁰ at temperature T obtained from n independent simulations, each with N_j configurations, is given by

$$P(E, T) = \frac{\sum_{i=1}^n H_i(E) \exp[E/k_B T]}{\sum_{j=1}^n N_j \exp[E/k_B T_j - f_j]}, \quad (2)$$

where

$$\exp[f_i] = \sum_E P(E, T_i). \quad (3)$$

The thermal average of a physical quantity A is then calculated by

$$\langle A(T) \rangle = \sum_E A P(E, T) / z(T), \quad (4)$$

in which

$$z(T) = \sum_E P(E, T). \quad (5)$$

Thermal averages of physical quantities are thus calculated as continuous functions of T , now the results should be valid over a much wider range of temperature than for any single histogram. The xy linear sizes $L = 20, 25, 30, \dots, 80$ have been used in our simulations. We have tested that all exponents do not change in the finite size scaling with $L \geq 30$. So most of results are shown for $L \geq 30$ except for ν where the lowest sizes $L = 20, 25$ can be used without modifying its value.

In practice, we use first the standard MC simulations to localize for each size the transition temperatures $T_0^E(L)$ for specific heat and $T_0^m(L)$ for susceptibility. The equilibrating time is from 200000 to 400000 MC steps/spin and the averaging time is from 500000 to 1000000 MC steps/spin. Next, we make histograms at 8 different temperatures $T_j(L)$ around the transition temperatures $T_0^{E,m}(L)$ with 2 millions MC steps/spin, after discarding 1 millions MC steps/spin for equilibrating. Finally, we make again histograms at 8 different temperatures around the new transition temperatures $T_0^{E,m}(L)$ with 2×10^6 and 4×10^6 MC steps/spin for equilibrating and averaging time, respectively. Such an iteration procedure gives extremely good results for systems studied so far. Errors shown in the following have been estimated using statistical errors, which are very small thanks to our multiple histogram procedure, and fitting errors given by fitting software.

We have calculated the averaged order parameter $\langle M \rangle$ (M : magnetization of the film), averaged total energy $\langle E \rangle$, specific heat C_v , susceptibility χ , first order cumulant of the energy C_U , and n^{th} order cumulant of the

order parameter V_n for $n = 1$ and 2 . These quantities are defined as

$$\langle E \rangle = \langle \mathcal{H} \rangle, \quad (6)$$

$$C_v = \frac{1}{k_B T^2} (\langle E^2 \rangle - \langle E \rangle^2), \quad (7)$$

$$\chi = \frac{1}{k_B T} (\langle M^2 \rangle - \langle M \rangle^2), \quad (8)$$

$$C_U = 1 - \frac{\langle E^4 \rangle}{3\langle E^2 \rangle^2}, \quad (9)$$

$$V_n = \frac{\partial \ln M^n}{\partial (1/k_B T)} = \langle E \rangle - \frac{\langle M^n E \rangle}{\langle M^n \rangle}. \quad (10)$$

Plotting these quantities as functions of T for system size (L, N_z) , we can identify the transition temperature by looking at their respective behavior (maxima of C_v and χ , ...). Note that the transition temperatures for these quantities coincide only at infinite L . For large values of L , the following scaling relations are expected (see details in Ref. 21):

$$V_1^{\max} \propto L^{1/\nu}, \quad V_2^{\max} \propto L^{1/\nu}, \quad (11)$$

$$C_v^{\max} = C_0 + C_1 L^{\alpha/\nu} \quad (12)$$

and

$$\chi^{\max} \propto L^{\gamma/\nu} \quad (13)$$

at their respective 'transition' temperatures $T_c(L)$, and

$$C_U = C_U[T_c(\infty)] + AL^{-\alpha/\nu}, \quad (14)$$

$$M_{T_c(\infty)} \propto L^{-\beta/\nu} \quad (15)$$

and

$$T_c(L) = T_c(\infty) + C_A L^{-1/\nu}, \quad (16)$$

where A , C_0 , C_1 and C_A are constants. We estimate ν independently from V_1^{\max} and V_2^{\max} . With this value we calculate γ from χ^{\max} and α from C_v^{\max} . Note that we can estimate $T_c(\infty)$ by using the last expression. Using $T_c(\infty)$, we can calculate β from $M_{T_c(\infty)}$. The Rushbrooke scaling law $\alpha + 2\beta + \gamma = 2$ is then in principle verified. Finally, using the hyperscaling relationship, we can estimate the "effective" dimension of thin films by $d_{\text{eff}} = (2 - \alpha)/\nu$ and the exponent η from the scaling law $\gamma = (2 - \eta)\nu$.

We note however that only ν is directly calculated from MC data. Exponent γ obtained from χ^{\max} and ν suffers little errors (systematic errors and errors from ν). Other exponents are obtained by MC data and several-step fitting. For example, to obtain α we have to fit C_v^{\max} of

Eq. 12 by choosing C_0 , C_1 and by using the value of ν . So in practice, in most cases, one calculates α or β from MC data and uses the Rushbrooke scaling law to calculate the remaining exponent. However, for our precise purpose we will show in the following the results of all exponents ν , γ , α and β calculated from MC data. We will show that the Rushbrooke scaling law is very well verified. The exponent α will allow us to estimate the effective dimension of the system.

III. RESULTS

We show now the results obtained by MC simulations with the Hamiltonian (1).

Let us show in Fig. 1 the layer magnetizations and their corresponding susceptibilities of the first three layers, in the case where $J_s = 1$. It is interesting to note that the surface layer is smaller than the interior layers, as it has been shown theoretically by the Green's function method a long time ago.^{15,16} The surface spins have smaller local field due to the lack of neighbors, so thermal fluctuations will reduce their magnetization with respect to the interior layers. The susceptibilities have their peaks at the same temperature, indicating a single transition.

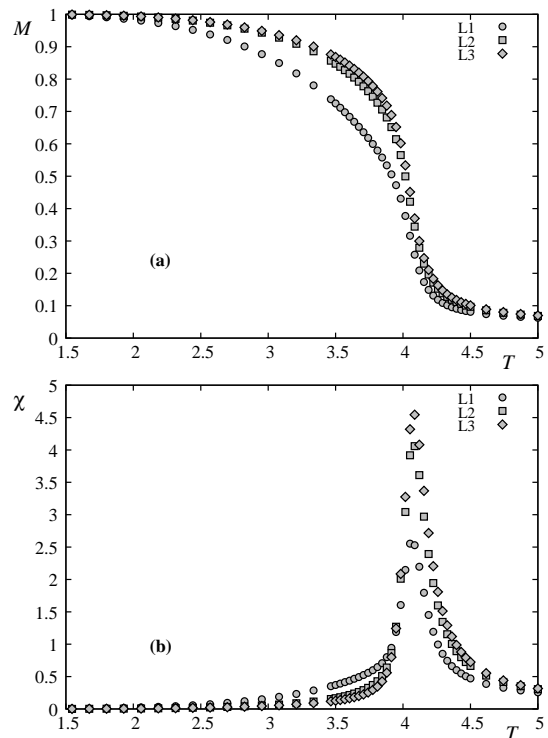


FIG. 1: Layer magnetizations (a) and layer susceptibilities (b) versus T with $N_z = 5$.

Figure 2 shows total magnetization of the film and the total susceptibility. This indicates clearly that there is only one peak as said above.

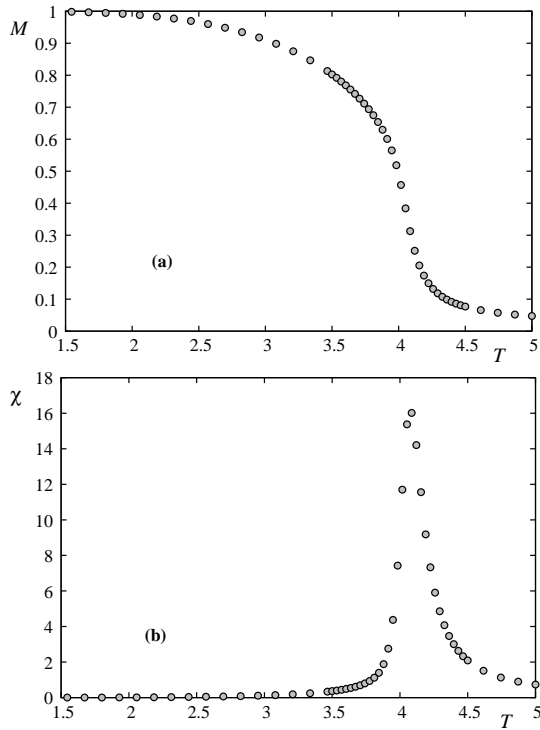


FIG. 2: Total magnetization (a) and total susceptibility (b) versus T with $N_z = 5$.

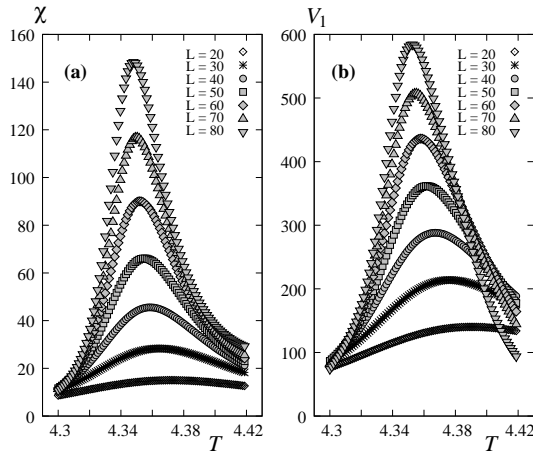


FIG. 3: (a) Susceptibility and (b) V_1 , as functions of T for several L with $N_z = 11$, obtained by multiple histogram technique.

Let us show now an example of excellent results obtained from multiple histograms described above. Figure 3 shows the susceptibility and the first derivative V_1 versus T around their maxima for several sizes.

We show in Fig. 4 the maximum of the first derivative of $\ln M$ with respect to $\beta = (k_B T)^{-1}$ versus L in the $\ln - \ln$ scale for several film thicknesses up to $N_z = 13$. From the slopes of these remarkably straight lines, we obtain $1/\nu$. We plot in Fig. 5 ν as a function of thickness N_z . We observe here a small but systematic de-

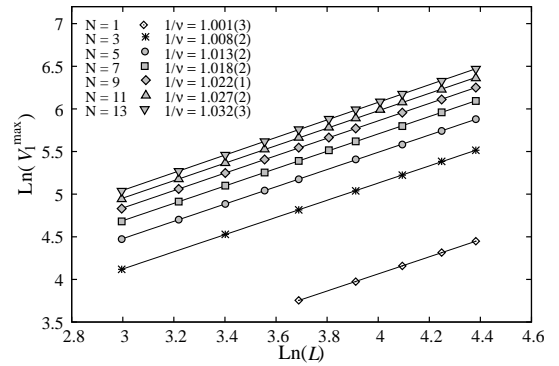


FIG. 4: Maximum of the first derivative of $\ln M$ versus L in the $\ln - \ln$ scale.

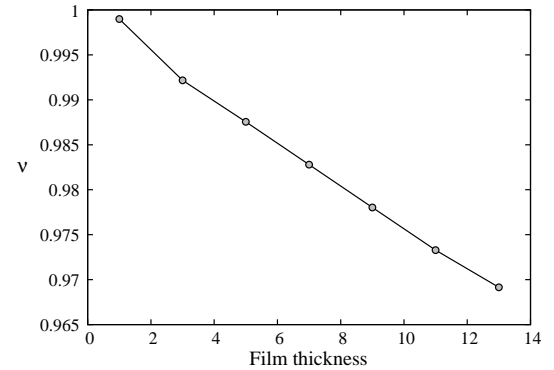


FIG. 5: ν versus N_z .

viation of ν from its 2D value ($\nu_{2D} = 1$) with increasing thickness. To show the precision of our method, we give here the results of $N_z = 1$. For $N_z = 1$, we have $1/\nu = 1.0010 \pm 0.0028$ which yields $\nu = 0.9990 \pm 0.0031$ and $\gamma/\nu = 1.7537 \pm 0.0034$ (see Figs. 6 and 7 below) yielding $\gamma = 1.7520 \pm 0.0062$. These results are in excellent agreement with the exact results $\nu_{2D} = 1$ and $\gamma_{2D} = 1.75$. The very high precision of our method is thus verified in the range of the system sizes used in the present work.

We show in Fig. 6 the maximum of the susceptibility versus L in the $\ln - \ln$ scale for film thicknesses up to $N_z = 13$. We have used only results of $L \geq 30$. Including $L = 20$ and 25 will result, unlike the case of ν , in a decrease of γ of about one percent for $N_z \geq 7$. From the slopes of these straight lines, we obtain the values of γ/ν . Using the values of ν obtained above, we deduce the values of γ which are plotted in Fig. 7 as a function of thickness N_z . Unlike the case of ν , we observe here a stronger deviation of γ from its 2D value (1.75) with increasing thickness. This finding is somewhat interesting: the magnitude of the deviation from the 2D value may be different from one critical exponent to another: $\simeq 3\%$ for ν and $\simeq 8\%$ for γ when N_z goes from 1 to 13. We will see below that β varies even more strongly.

At this stage, a natural question arises: does the ab-

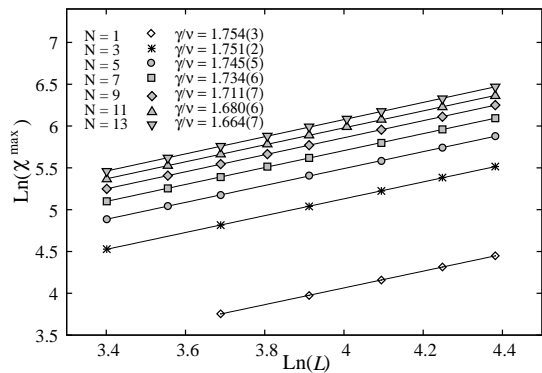


FIG. 6: Maximum of susceptibility versus L in the $\ln - \ln$ scale.

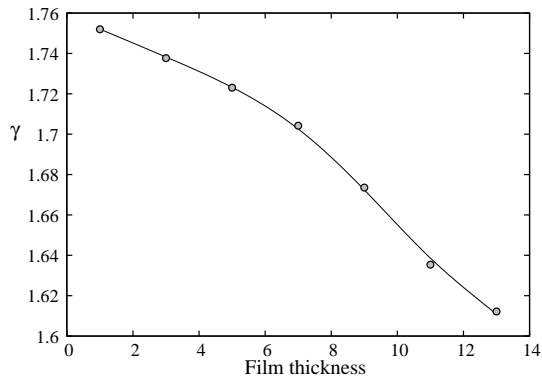


FIG. 7: γ versus N_z .

sence of PBC in the z direction cause these deviations of the critical exponents? The answer is no: we have calculated ν and γ for $N_z = 5$ in both cases: with and without PBC in the z direction. The results show no significant difference between the two cases as seen in Figs. 8 and 9. We have found the same thing with $N_z = 11$ shown in Figs. 10 and 11. So, we conclude that the fixed thickness will result in the deviation of the critical exponents, not from the absence of the PBC. This is somewhat surprising since we thought, incorrectly, that the PBC should mimic the infinite dimension so that we should obtain the 3D behavior when applying the PBC. As will be seen below, the 3D behavior is recovered only when the finite size scaling is applied in the z direction at the same time in the xy plane. To show this, we plot in Figs. 12 and 13 the results for the 3D case. Even with our modest sizes (up to $L = N_z = 21$, since it is not our purpose to treat the 3D case here), we obtain $\nu = 0.613 \pm 0.005$ and $\gamma = 1.250 \pm 0.005$ very close to their 3D best known values $\nu_{3D} = 0.6289 \pm 0.0008$ and $\gamma_{3D} = 1.2390 \pm 0.0025$ obtained by using $24 \leq L \leq 96$).²⁴

Let us discuss on the deviation of the critical exponents due to the film finite thickness. For second-order transitions, theoretical arguments, such as those from the renormalization group, say that the correlation length in the direction perpendicular to the film is finite, hence it

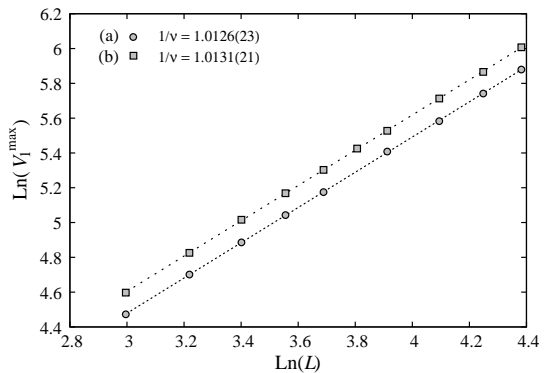


FIG. 8: Maximum of the first derivative of $\ln M$ versus L in the $\ln - \ln$ scale for $N_z = 5$ (a) without PBC in z direction (b) with PBC in z direction.

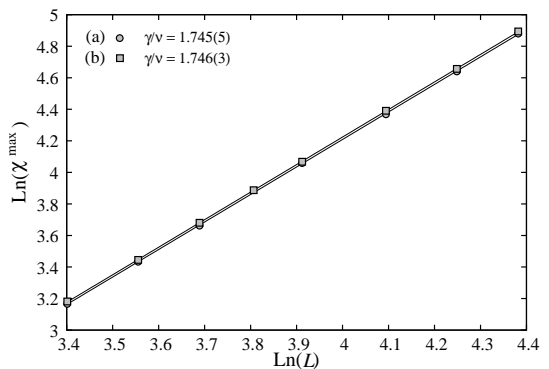


FIG. 9: Maximum of susceptibility versus L in the $\ln - \ln$ scale for $N_z = 5$ (a) without PBC in z direction (b) with PBC in z direction. The points of these cases cannot be distinguished in the figure scale.

is irrelevant to the criticality, the film should have the 2D character as long as N_z is finite. We have seen above that this is not the case here. The deviation begins slowly as soon as N_z departs from 1. A possible cause for the deviation is from the spatially non uniform correlation: the correlation in a xy plane depends obviously on its position with respect to the surface layer. On and near the surface, the spins suffer thermal fluctuations more strongly than the interior spins so there is no reason why all planes should have the same in-plane correlation behavior even when there is no separate surface transition as in the case $J_s = 1$ studied here. Due to this spatially non uniform fluctuations, we believe that near the phase transition, there are simultaneously several correlation lengths which give rise to a kind of "effective" critical exponents obtained above. Loosely speaking, we can say in another manner that because of its spatial non uniformity, the correlation in the direction perpendicular to the film cannot be separately summed up, it interacts with the xy correlation giving rise to "effective" critical exponents observed in our simulations. In other words, the finite thickness makes the dimension of the system some-

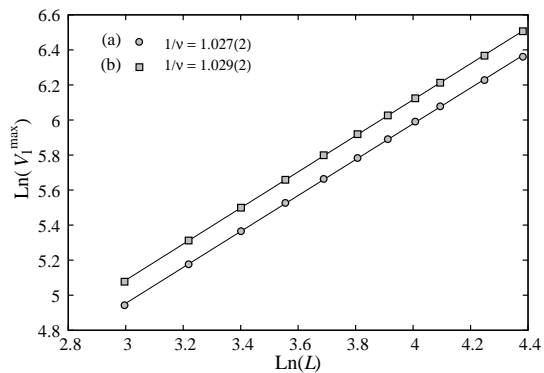


FIG. 10: Maximum of the first derivative of $\ln M$ versus L in the $\ln - \ln$ scale for $N_z = 11$ (a) without PBC in z direction (b) with PBC in z direction.

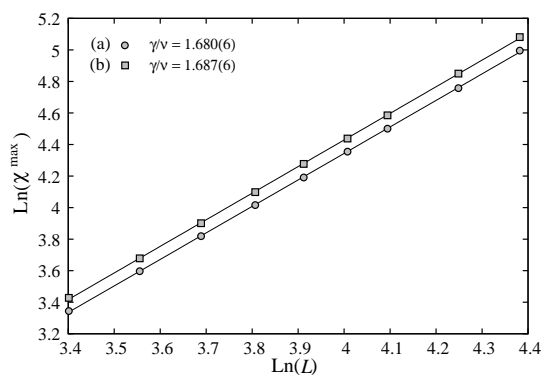


FIG. 11: Maximum of susceptibility versus L in the $\ln - \ln$ scale for $N_z = 11$ (a) without PBC in z direction (b) with PBC in z direction.

thing between 2 and 3. Before showing this "effective" dimension, we show in Fig. 14 the maximum of C_v^{\max} versus L for $N_z = 1, 3, 5, \dots, 13$. Note that for each N_z we had to look for C_0 , C_1 and α/ν which give the best fit with data of C_v^{\max} . Due to the fact that there are several parameters which can induce a wrong combination

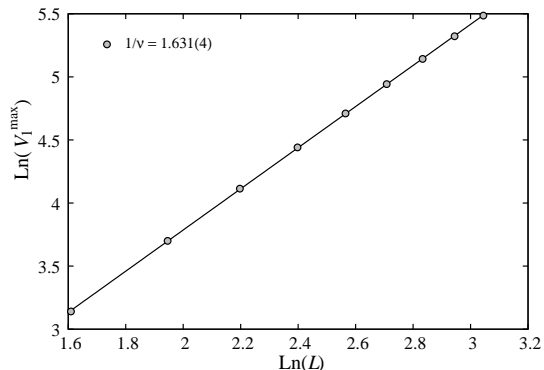


FIG. 12: Maximum of the first derivative of $\ln M$ versus L in the $\ln - \ln$ scale for 3D case.

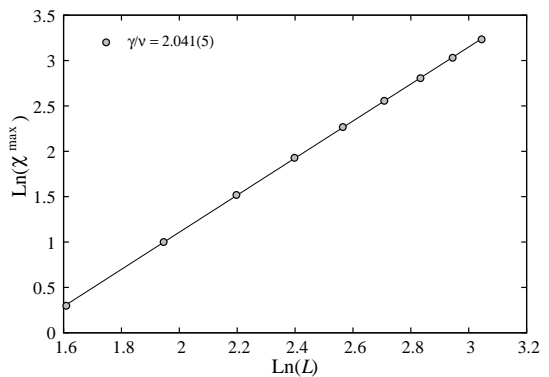


FIG. 13: Maximum of susceptibility versus L in the $\ln - \ln$ scale for 3D case.

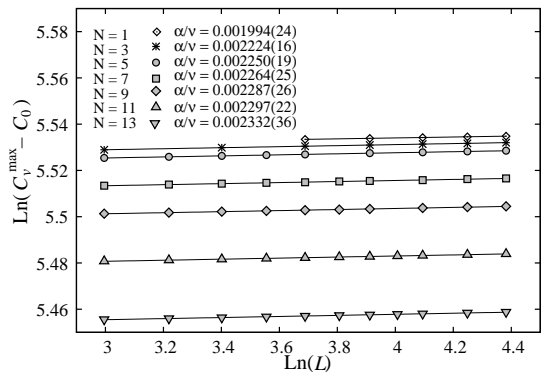


FIG. 14: $\ln(C_v^{\max} - C_0)$ versus $\ln L$ for $N_z = 1, 3, 5, \dots, 13$. The slope gives α/ν (see Eq. 12).

of them, we impose that α should satisfied the condition $0 \leq \alpha \leq 0.11$ where the lower limit of α corresponds to the value of 2D case and the upper limit to the 3D case. In doing so, we get very good results shown in Fig. 14. From these ratios of α/ν we deduce α for each N_z . The values of α are shown in Table I for several N_z .

It is interesting to show now the effective dimension of thin film discussed above. Replacing the values of α obtained above in $d_{\text{eff}} = (2 - \alpha)/\nu$ we obtain d_{eff} shown in Fig. 15.

We note that d_{eff} is very close to 2. It varies from 2 to $\simeq 2.061$ for N_z going from 1 to 13. The 2D character is thus dominant even with larger N_z . This supports the idea that the finite correlation in the z direction, though qualitatively causing a deviation, cannot strongly alter the 2D critical behavior. This point is interesting because, as said earlier, some thermodynamic properties may show already their 3D values at a thickness of about a few dozens of layers, but not the critical behavior. To show an example of this, let us plot in Fig. 16 the transition temperature at $L = \infty$ for several N_z , using Eq. 16 for each given N_z . As seen, $T_c(\infty)$ reaches already $\simeq 4.379$ at $N_z = 13$ while its value at 3D is 4.51.²⁴ A rough extrapolation shows that the 3D values is attained for $N_z \simeq 25$ while the critical exponents at this thickness

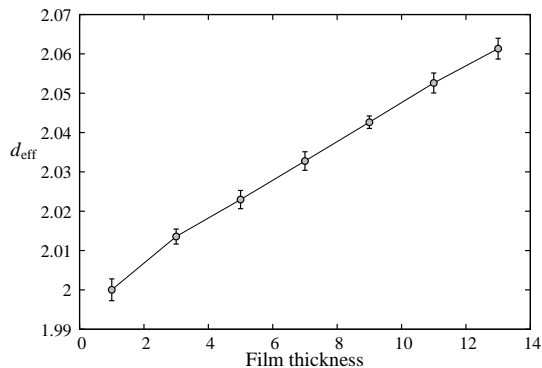


FIG. 15: Effective dimension of thin film as a function of thickness.

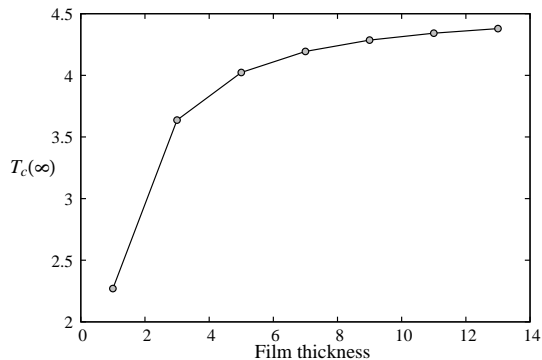


FIG. 16: Critical temperature at infinite L as a function of the film thickness.

IV. CONCLUDING REMARKS

We have considered a simple system, namely the Ising model on a simple cubic thin film, in order to clarify the point whether or not there is a continuous deviation of the 2D exponents with varying film thickness. From results obtained by the highly accurate multiple histogram technique shown above, we conclude that the critical exponents in thin films show a continuous deviation from their 2D values as soon as the thickness departs from 1. We believe that this deviation stems from deep physical mechanisms, not from the calculation method used here. We would like moreover to emphasize some additional interesting observations:

1. The deviations of the exponents from their 2D values are very different in magnitude: while ν and α vary very little over the studied range of thickness, γ and specially β suffer stronger deviations
2. With a fixed thickness (> 1), the same critical exponents are observed, within errors, in simulations with or without periodic boundary condition in the z direction
3. To obtain the 3D behavior, finite size scaling should be applied simultaneously in the three directions. If we

are far away from the 3D ones.

We give the precise values of $T_c(\infty)$ for each thickness. For $N_z = 1$, we have $T_c(\infty) = 2.2701 \pm 0.0003$ from T_c of specific heat and 2.2697 ± 0.0005 from T_c of susceptibility. From these we have $T_c(\infty) = 2.2699 \pm 0.0005$. Note that the exact value of $T_c(\infty)$ is 2.26919 by solving the equation $\sinh^2(2J/T_c) = 1$. Again here, the excellent agreement of our result shows the efficiency of the multiple histogram technique as applied in the present paper. The values of $T_c(\infty)$ for other N_z are summarized in Table I.

Calculating now $M(L)$ at these values of $T_c(\infty)$ and using Eq. 15, we obtain β/ν for each N_z . For $N_z = 1$, we have $\beta/\nu = 0.1268 \pm 0.0022$ which yields $\beta = 0.1266 \pm 0.0049$ which is in excellent agreement with the exact result (0.125). Note that if we calculate β from $\alpha + 2\beta + \gamma = 2$, then $\beta = (2 - 1.75198 - 0.00199)/2 = 0.12302 \pm 0.0035$ which is in good agreement with the direct calculation within errors. We show in Fig. 17 the values of β obtained by direct calculation using Eq. 15. Note that the deviation of β from the 2D value when N_z varies from 1 to 13 represents about 60%. Note that the 3D value of β is 0.3258 ± 0.0044 .²⁴

Finally, for convenience, let us summarize our results in Table I for $N_z = 1, 3, \dots, 13$. Due to the smallness of α , its value is shown with 5 decimals without rounding.

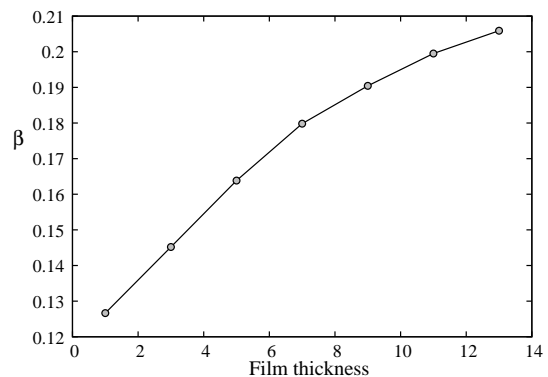


FIG. 17: Critical exponent β versus the film thickness obtained by using Eq. 15.

do not apply the scaling in the z direction, we will not obtain 3D behavior even with a very large, but fixed, thickness and even with periodic boundary condition in the z direction

4. With regard to the critical behavior, thin films behave as systems with effective dimensions between 2 and 3, depending on the film thickness. Note however that,

TABLE I: Critical exponents, effective dimension and critical temperature at infinite xy limit as obtained in this paper.

N_z	ν	γ	α	β	d_{eff}	$T_c(\infty)$
1	0.9990 ± 0.0028	1.7520 ± 0.0062	0.00199 ± 0.00279	0.1266 ± 0.0049	2.0000 ± 0.0028	2.2699 ± 0.0005
3	0.9922 ± 0.0019	1.7377 ± 0.0035	0.00222 ± 0.00192	0.1452 ± 0.0040	2.0135 ± 0.0019	3.6365 ± 0.0024
5	0.9876 ± 0.0023	1.7230 ± 0.0069	0.00222 ± 0.00234	0.1639 ± 0.0051	2.0230 ± 0.0023	4.0234 ± 0.0028
7	0.9828 ± 0.0024	1.7042 ± 0.0087	0.00223 ± 0.00238	0.1798 ± 0.0069	2.0328 ± 0.0024	4.1939 ± 0.0032
9	0.9780 ± 0.0016	1.6736 ± 0.0084	0.00224 ± 0.00161	0.1904 ± 0.0071	2.0426 ± 0.0016	4.2859 ± 0.0022
11	0.9733 ± 0.0025	1.6354 ± 0.0083	0.00224 ± 0.00256	0.1995 ± 0.0088	2.0526 ± 0.0026	4.3418 ± 0.0032
13	0.9692 ± 0.0026	1.6122 ± 0.0102	0.00226 ± 0.00268	0.2059 ± 0.0092	2.0613 ± 0.0027	4.3792 ± 0.0034

except a strong deviation of γ , other exponents stay near their 2D limit even with a large thickness, while non critical thermodynamic properties may attain 3D behaviors at a thickness of about a few dozens atomic layers.

To conclude, we hope that the numerical results shown in this paper will stimulate more theoretical analysis in search for the origin of the continuous variation of the critical exponents with changing thickness. It should be also desirable to study more cases to clarify the role of

thickness on the transition behavior of very thin films, in particular the effect of the film thickness on the bulk first-order transition.

One of us (VTN) thanks the "Asia Pacific Center for Theoretical Physics" (South Korea) for a financial post-doc support and hospitality during the period 2006-2007 where part of this work was carried out. The authors are grateful to Yann Costes of the University of Cergy-Pontoise for technical help in parallel computation.

-
- ¹ A. Zangwill, *Physics at Surfaces*, Cambridge University Press (1988).
- ² *Ultrathin Magnetic Structures*, vol. I and II, J.A.C. Bland and B. Heinrich (editors), Springer-Verlag (1994).
- ³ M. N. Baibich, J. M. Broto, A. Fert, F. Nguyen Van Dau, F. Petroff, P. Etienne, G. Creuzet, A. Friederich and J. Chazelas, *Phys. Rev. Lett.* **61**, 2472 (1988).
- ⁴ P. Grunberg, R. Schreiber, Y. Pang, M. B. Brodsky and H. Sowers, *Phys. Rev. Lett.* **57**, 2442 (1986); G. Binash, P. grunberg, F. Saurenbach and W. Zinn, *Phys. Rev. B* **39**, 4828 (1989).
- ⁵ A. Barthélémy et al, *J. Mag. Mag. Mater.* **242-245**, 68 (2002).
- ⁶ See review by E. Y. Tsymbal and D. G. Pettifor, *Solid State Physics* (Academic Press, San Diego), Vol. 56, pp. 113-237 (2001).
- ⁷ K. Binder, in *Phase Transitions and Critical Phenomena*, ed. by C. Domb, J.L. Lebowitz (Academic, London, 1983) vol. 8.
- ⁸ H.W. Diehl, in *Phase Transitions and Critical Phenomena*, ed. by C. Domb, J.L. Lebowitz (Academic, London, 1986) vol. 10, H.W. Diehl, *Int. J. Mod. Phys. B* **11**, 3503 (1997).
- ⁹ L. Onsager, *Phys. Rev.* **65**, 117 (1944).
- ¹⁰ N. D. Mermin and H. Wagner, *Phys. Rev. Lett.* **17**, 1133 (1966).
- ¹¹ J. Zinn-Justin, *Quantum Field Theory and Critical Phenomena*, Oxford University Press (4th edition - 2002).
- ¹² H. T. Diep, *Phys. Rev. B* **40**, 4818 (1989).
- ¹³ H. T. Diep, *Phys. Rev. B* **43**, 8509 (1991).
- ¹⁴ See V. Thanh Ngo, H. Viet Nguyen, H. T. Diep and V. Lien Nguyen, *Phys. Rev. B.* **69**, 134429 (2004) and references on magnetic multilayers cited therein.
- ¹⁵ H. T. Diep, J.C. S. Levy and O. Nagai, *Phys. Stat. Solidi (b)* **93**, 351 (1979).
- ¹⁶ H. T. Diep, *Phys. Stat. Solidi (b)*, **103**, 809 (1981).
- ¹⁷ D. P. Landau and K. Binder, *Phys. Rev. B* **41**, 4786 (1990).
- ¹⁸ D. P. Landau and K. Binder, *Phys. Rev. B* **41**, 4633 (1990).
- ¹⁹ A. M. Ferrenberg and R. H. Swendsen, *Phys. Rev. Lett.* **61**, 2635 (1988).
- ²⁰ A. M. Ferrenberg and R. H. Swendsen, *Phys. Rev. Lett.* **63**, 1195 (1989).
- ²¹ A. Bunker, B. D. Gaulin, and C. Kallin, *Phys. Rev. B* **48**, 15861 (1993).
- ²² See V. Thanh Ngo and H. T. Diep, *Phys. Rev. B.* **75**, 035412 (2007) and references on surface effects cited therein.
- ²³ See V. Thanh Ngo and H. T. Diep, *cond-mat/arXiv:0705.1169*.
- ²⁴ A. M. Ferrenberg and D. P. Landau, *Phys. Rev. B* **44**, 5081 (1991).